Electronic Supplementary Information

Interfacial restructuration of carbon nitride polymers for visible-light photocatalysis

*Feng Lin, Zihao Yu, Xinchen Wang**

State Key Laboratory of Photocatalysis on Energy and Environment, College of Chemistry, Fuzhou University, Fuzhou 350002, People's republic of China

Email: xcwang@fzu.edu.cn

Experimental section

Materials. 3,5-Dibromobenzoic acid, triethylamine, 1,4-Phenylenediboronic acid, 1,3,6,8-tetrabromopyrene, 4,4'-dibromo-2,2'-bipyridy, $SOCl_2$ and $Pd(PPh_3)_4$ are all of analytic grade and used without further modification or purification. N,N-dimethylformamide was purified by distillation under reduced pressure after drying with diphosphorus pentaoxide; CH_2Cl_2 and ethanol were purified by distillation with calcium hydride, which were all strict in dehydration treatment.

PCN. The polymeric carbon nitride was synthesized as described previously.[1]

Covalence bonds bridged PCN (CCN): A certain amount of 3,5-Dibromobenzoic acid was dissolved in $SOCl_2$ solution with few drops of anhydrous THF and refluxed for three hours under dried N_2. After cool to the room temperature, excessive thionyl chloride was removed at moisture-free and vacuo conditions. Dibromobenzoic acid chloride was slowly dropped into dried CH_2Cl_2 dispersing PCN powder under 0°C with equivalent of triethylamine. After 5h, the yellowishandgreen precipitates were obtained by rotary evaporation and centrifugal separation with the absolutely fresh anhydrous ethanol solution and water, then dried at 60 ºC for 24h.

Hydrogen bonds decorated polymeric carbon nitride (HCN): Firstly, dispersed

PCN powder into the absolutely fresh anhydrous ethanol solution, with monodispersed 3,5-Dibromobenzoic acid (2mmol/L) for 24h at room temperature. Then, centrifuged with absolutely fresh anhydrous ethanol solution and dried.

CCN-EG and HCN-EG: A three necked flask equipped with magnetic stir bar was charged with the mixtures of 1,4-Phenylenediboronicv acid (1mmol), $Pd(PPh_3)_4$ (1.2mol%), 1,3,6,8-tetrabromopyrene (0.4mmol), 4,4'-dibromo-2,2'-bipyridy (0.15mmol) and CCN (0.5g) under dried N_2 atmosphere. The K_2CO_3 aqueous solution and N,N-dimethylformamide were slowly added into the above reactor under vigorous stirring; then, refluxed until the reaction was complete which was judged by the thin layer chromatography (TLC) analysis. After cooling to the room temperature, the strong yellowish green precipitate were purification with H_2O and methanol several times and further extracted with tetrahydrofuran and methanol by Soxhlet for 48h, respectively. The product was dried under reduce pressure and further dried in the vacuum oven at 60 ºC for 24h. The product is about 73.5% and 67.2% yield for CCN-EG and HCN-EG compared with the bulk PCN.

Characterization: The C *K*-edge and N *K*-edge X-ray absorption near-edge spectra (XANES) were measured at BL12B-a beamline of National Synchrotron Radiation Laboratory (NSRL, China) in the total electron yield (TEY) mode by collecting the sample drain current under a vacuum better than 5×10^{-8} Pa. The beam from the bending magnet was monochromatized utilizing a varied linespacing plane grating and refocused by a toroidal mirror. The energy range is 100–1000 eV with an energy resolution of ca. 0.2 eV. X-ray diffraction (XRD) measurements were performed at Bruker D8 Advance diffractometer equipped with monochromatic Cu Kα radiation (λ=1.5418Å). Scanning electron microscope (SEM) images were conducted on a LEO Gemini 1530 (Carl Zeiss AG, Germany) using an in lens SE detector. Fourier transformed infrared (FTIR) spectra were recorded using a Nicolet Magna 670 FTIR spectrometer. The solid-state ^{13}C nuclear magnetic resonance (NMR) spectra were recorded on a Bruker Advance III 500 spectrometer. Transmission electron microscopy (TEM) was performed on a FEI Tencai 20 microscope. The photocurrent

performance analysis was performed using a BioLogic VSP-300 electrochemical system. The nitrogen adsorption–desorption isotherms were collected at 77 K using a Micromeritics ASAP 2020 surface area and porosity analyzer. The X-ray photoelectron (XPS) spectra were carried out on an ESCALAB 250 (Thermo Fisher Scientific) operating with Al Kα radiation (hυ=1486.6 eV; analysed area = 600 μm^2). The base pressure of the analyzer chamber was around 5×10^{-8} Pa. An elemental surface analysis was first executed, for each sample, in the range of 0–1200 eV with Fixed Retard Ratio mode. Raman spectroscopic measurements were performed on a Renishaw in Via Raman System 1000 with a 325 nm Nd:YAG excitation source at room temperature.

Photocatalytic HER Test. Hydrogen evolution reactions were carried out in a closed glass gas system where is connected to a Pyrex top-irradiation reaction vessel. Firstly, 50 mg of catalyst powders were dispersed in an aqueous solution (100mL) with 10mL sacrificial agent and 3wt% Pt with H_2PtCl_6. After removing air completely, the reaction solution was irradiated with a 300W Xeon lamp with the working current of 15A (Shenzhen ShengKang Technology Co., Ltd, China, LX300F). In order to rule out the short-pass light, the long-pass cut-off filter was applied to correct the incident light. The evolved gases were analyzed by gas chromatography equipped with a thermal conductive detector (TCD).

Photocatalytic CO_2 reduction. 30mg catalyst, 1mL triethanolamine (TEOA) and 1μmol $CoCl_2$, 15mg 2,2-bipyridine, 5mL acetonitrile were added to the reactor, respectively. After degassing and backfilling with pure CO_2, the reaction was carried out with 300W Xe lamp equipped with a 420nm cut-off filter and maintained at 30°C. After reaction, the gases were analyzed by using gas chromatography.

The apparent quantum yield (AQY) measurement. The AQY for hydrogen generations were carried out by using monochromatic LED lamps with band pass filter of 420 ± 4.6, 470 ± 4.4, 490 ± 3.8, 520 ± 4.0, respectively. The intensity of each

top-irradiation LED lamps were 14.3, 11.2, 7.6, 2.9 mW cm^{-1} which is determinate by ILT 950 spectroradiometer. The effective irradiation area was controlled as 9 cm^2(3×3 cm^2). Since an average of one hour hydrogen produced, the AQY was calculated as follow:

$$AQY = \frac{N_e}{N_p} \times 100\% = \frac{2 \times h \times c \times M \times N_A}{S \times P \times \lambda \times t} \times 100\%$$

Where, h refers to the Planck constant, c is the speed of light, M is behalf of the total hydrogen generation in one hour, N_A is the Avogadro constant, S is the effective irradiation area, P is the intensity of fixed irradiation light, t is the reaction time of hydrogen evolution reaction, λ just is the wavelength of the irradiation light.

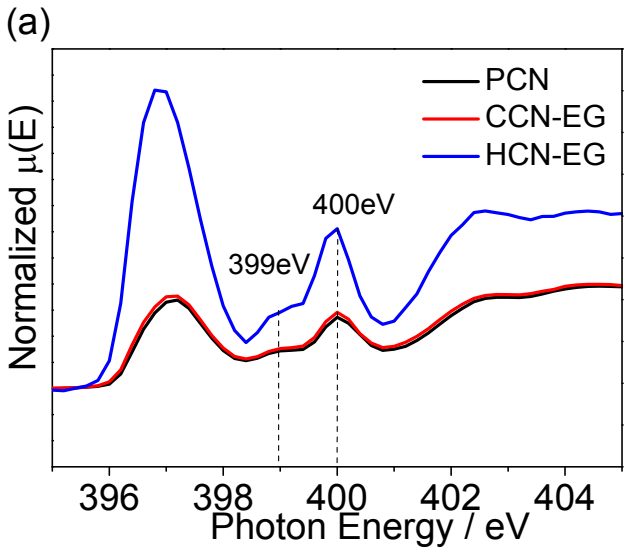

Fig. S1 The enlarged N *K*-edge for PCN, CCN-EG and HCN-EG.

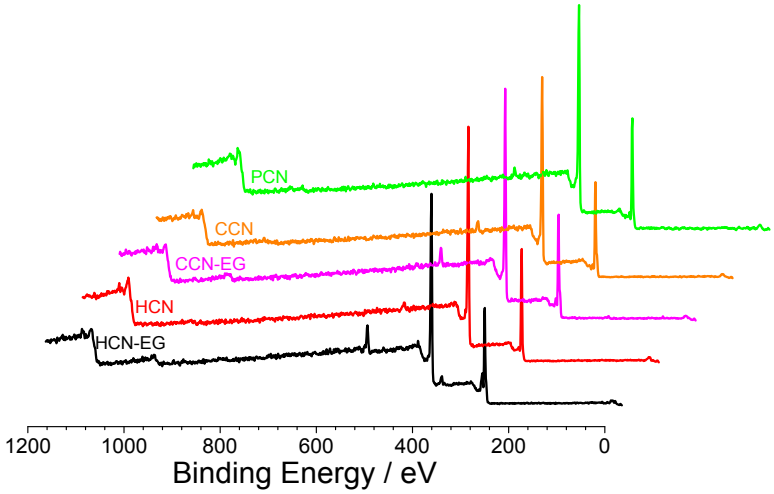

Fig. S2 Representative XPS survey spectra PCN, CCN, CCN-EG, HCN and HCN-EG.

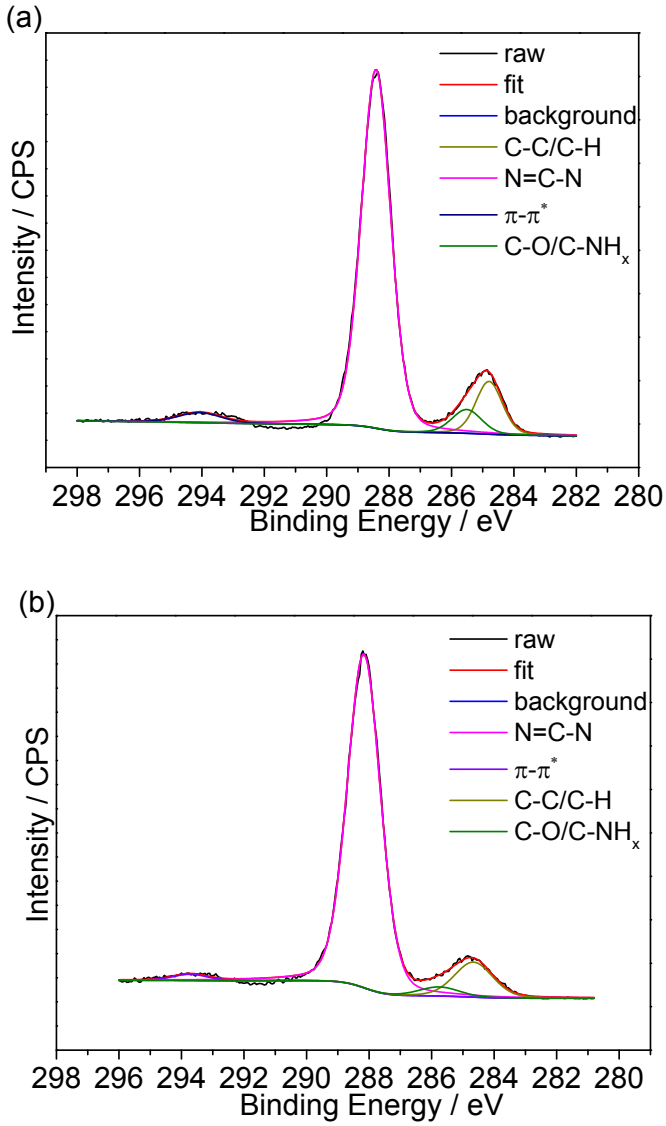

Fig. S3. The C1s XPS of CCN (a) and HCN(b).

Table S1 The present chemical environments, binding energy and their corresponding relative bond contents of C1s for samples.

Sample	Chemical states	Binding energy (eV)	Cont.%
PCN	C-C/C-H	284.8	6.05
	N=C-N	288.3	93.95
	π-π*	294.0	--
CCN	C-C/C-H	284.8	11.04
	C-O/C-NH_x	285.5	5.60
	N=C-N	288.4	83.36
	π-π*	294.1	--
HCN	C-C/C-H	284.7	10.52
	C-O/C-NH_x	285.8	2.79
	N=C-N	288.2	86.70
	π-π*	293.7	--
CCN-EG	C-C/C-H	284.8	10.75
	C-O/C-NH_x	285.5	5.12
	N=C-N	288.4	78.41
	π-π*	293.2	--
HCN-EG	C-C/C-H	284.8	10.81
	C-O/C-NH_x	285.9	2.02
	N=C-N	288.3	71.70
	π-π*	293.1	--

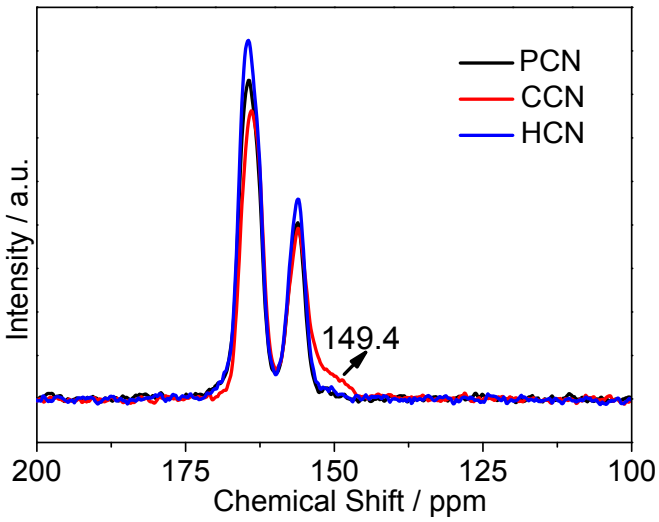

Fig. S4 the solid state ^{13}C NMR results of PCN, CCN and HCN

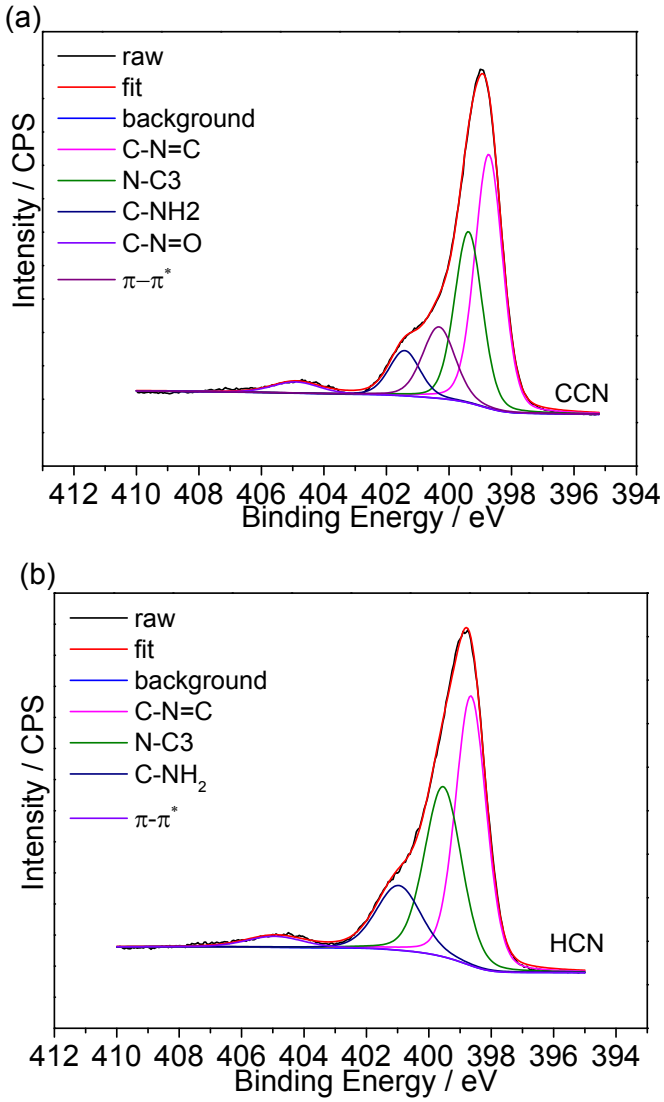

Fig. S5 The N1s XPS of CCN and HCN.

Table S2. The present chemical environments, binding energy and their corresponding relative bond contents of N1s for samples.

Sample	Chemical states	Binding energy (eV)	Cont.%
PCN	C-N=C	398.6	49.57
	N-C3	399.4	30.53
	C-NHx	400.8	19.89
	π-π*	404.6	--
CCN	C-N=C	398.7	45.58
	N-C3	399.4	30.45
	C-NHx	400.3	15.03
	C-N=O	401.4	8.92
	π-π*	404.8	--
HCN	C-N=C	398.6	47.52
	N-C3	399.5	35.9
	C-NHx	401.0	16.48
	π-π*	404.9	--
CCN-EG	C-N=C	398.5	35.86
	N-C3	399.1	29.44
	C-NHx	399.9	23.55
	C-N=O	401.2	11.14
	π-π*	405.1	--
HCN-EG	C-N=C	398.7	53.84
	N-C3	399.6	33.68
	C-NHx	401.0	12.47
	π-π*	405.4	--

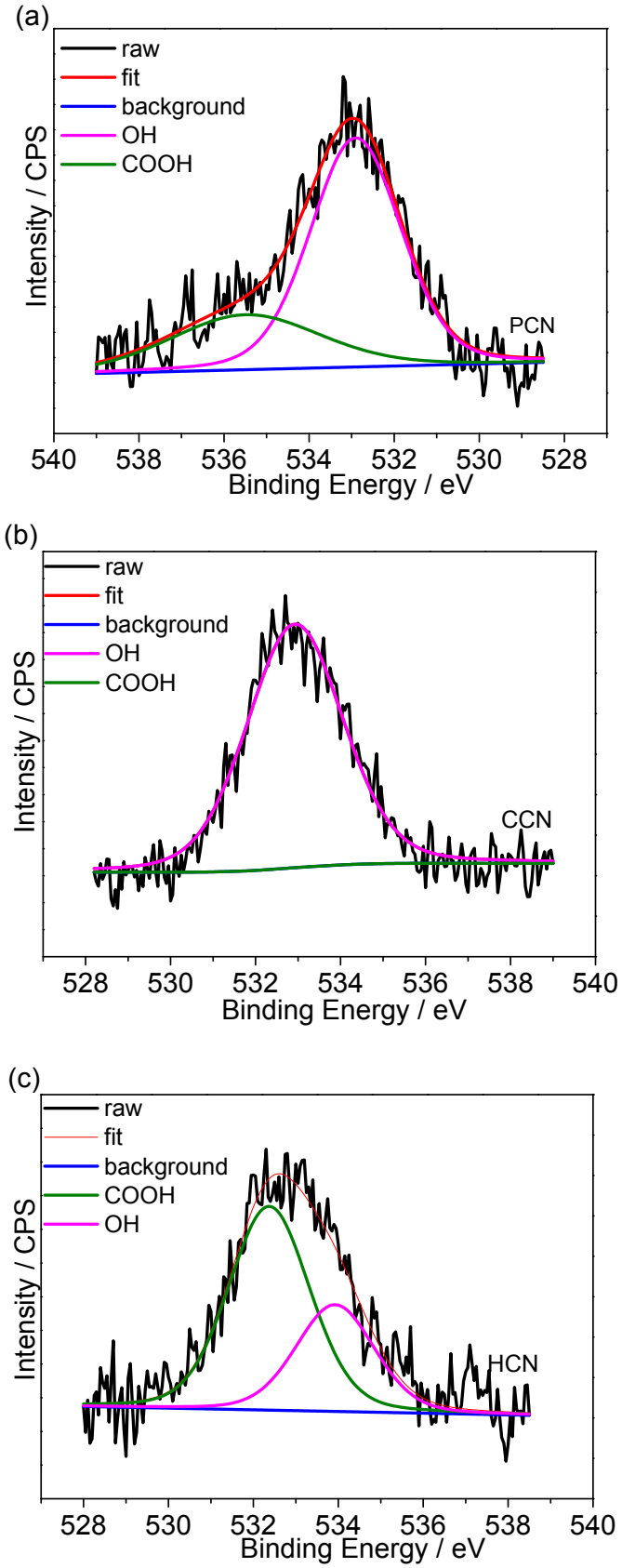
(a)
raw
fit
background
OH
COOH
Intensity / CPS
PCN
540
538
536
534
532
530
528
Binding Energy / eV
(b)
raw
fit
background
OH
COOH
Intensity / CPS
CCN
528
530
532
534
536
538
540
Binding Energy / eV
(c)
raw
fit
background
COOH
OH
Intensity / CPS
HCN
528
530
532
534
536
538
540
Binding Energy / eV

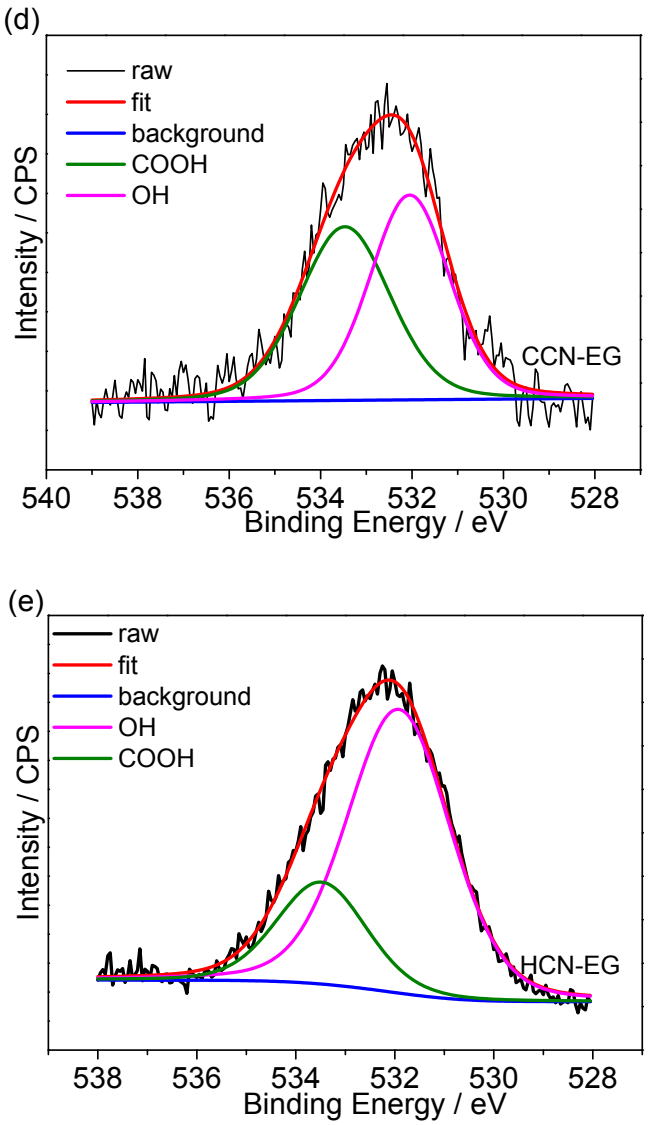

Fig. S6 The O1s XPS of PCN, CCN, HCN, CCN-EG and HCN-EG.

Table S3. The present chemical environments, binding energy and their corresponding relative bond contents of O1s for samples.

Sample	Chemical states	Binding energy (eV)	Cont.%
PCN	COOH	535.5	28.39
	C-OH	532.9	71.61
CCN	COOH	--	--
	C-OH	532.9	100
HCN	COOH	533.9	33.58
	C-OH	532.3	66.42
CCN-EG	COOH	533.5	49.27
	C-OH	532.0	50.73
HCN-EG	COOH	533.5	76.13
	C-OH	531.9	23.87

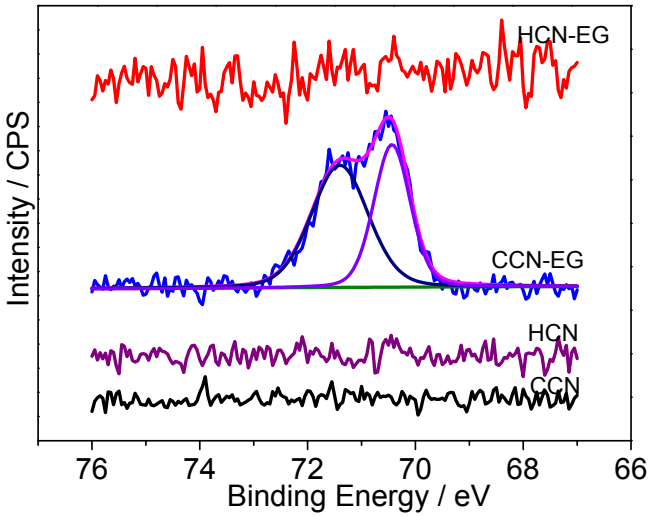

Fig. S7 The Br3d XPS of CCN, HCN, CCN-EG and HCN-EG.

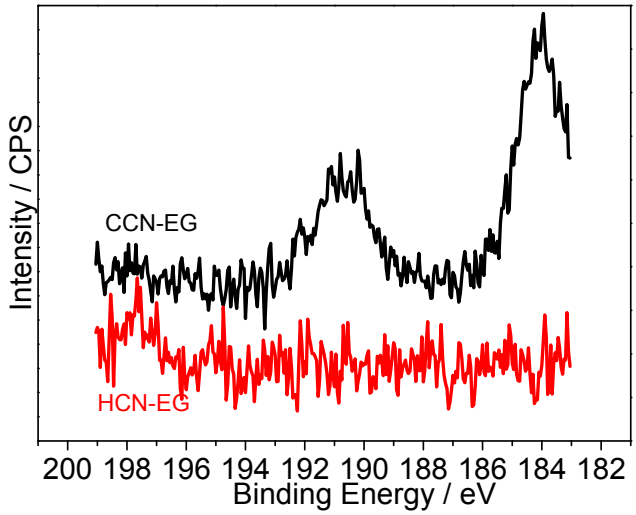

Fig. S8 The B1s XPS of CCN-EG and HCN-EG.

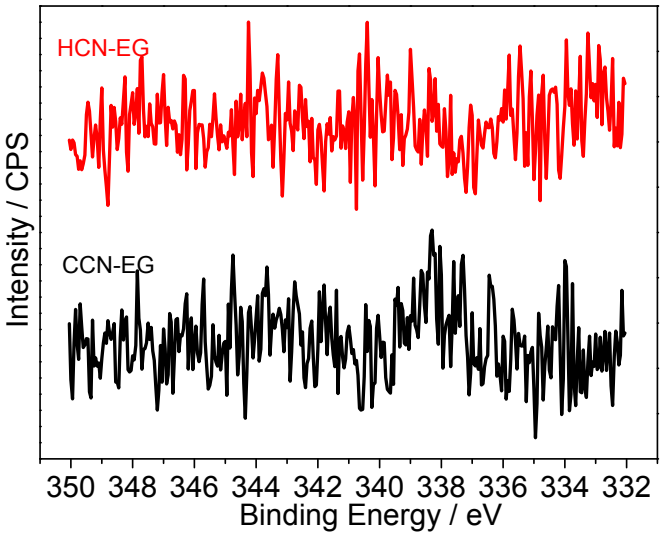

Fig. S9 The Pd3d XPS of CCN-EG and HCN-EG.

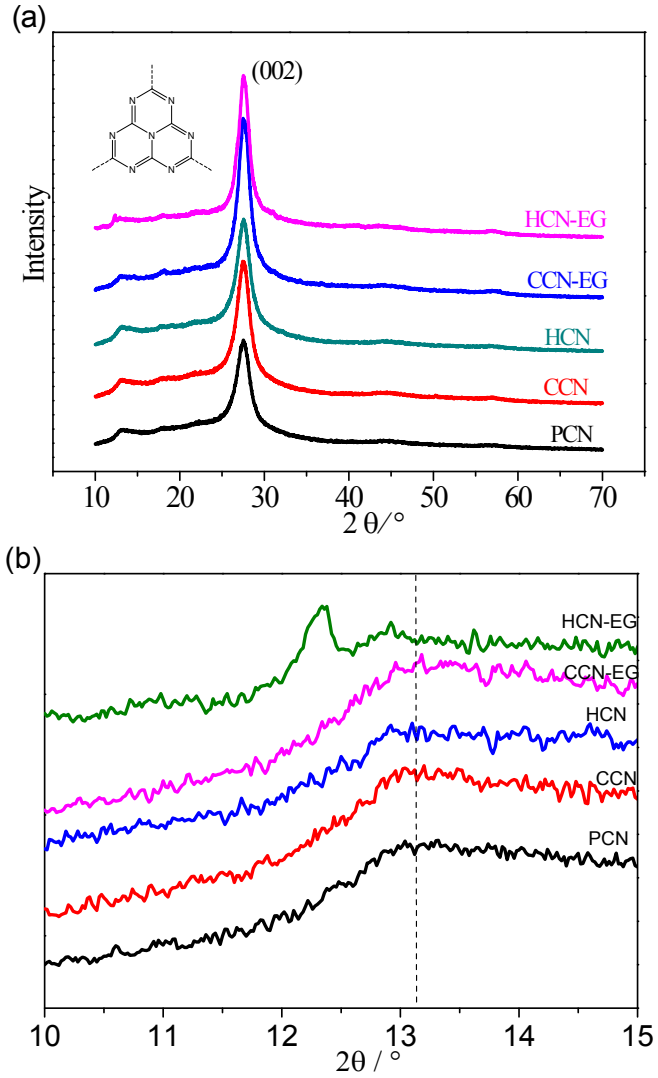

Fig. S10 The XRD results of catalysts

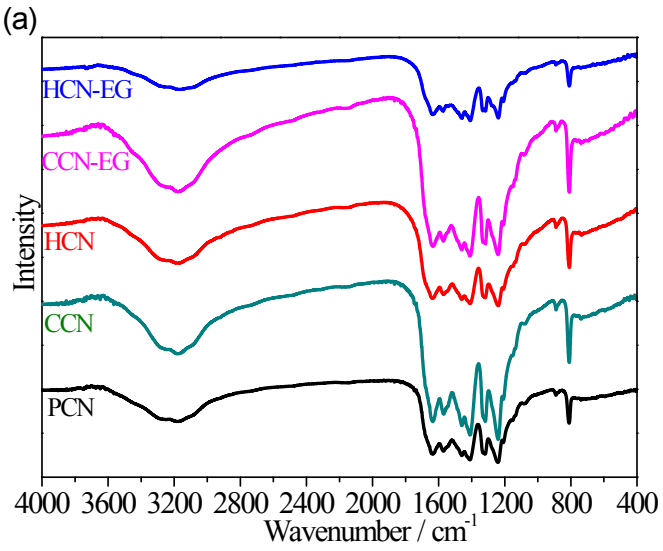

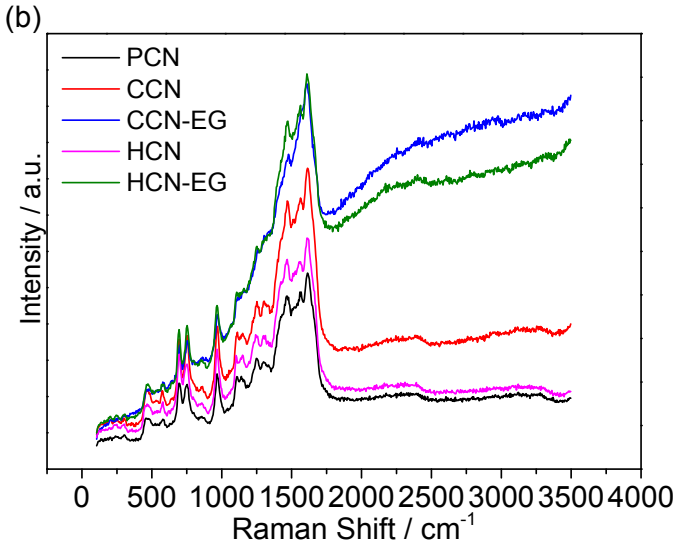

Fig. S11 The IR and Raman results of samples.

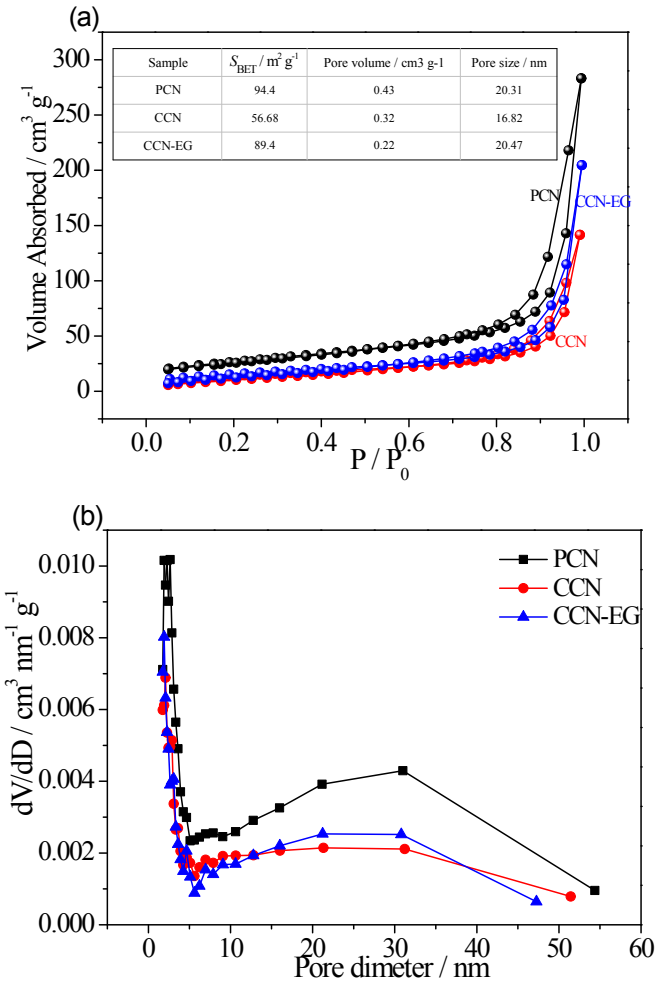

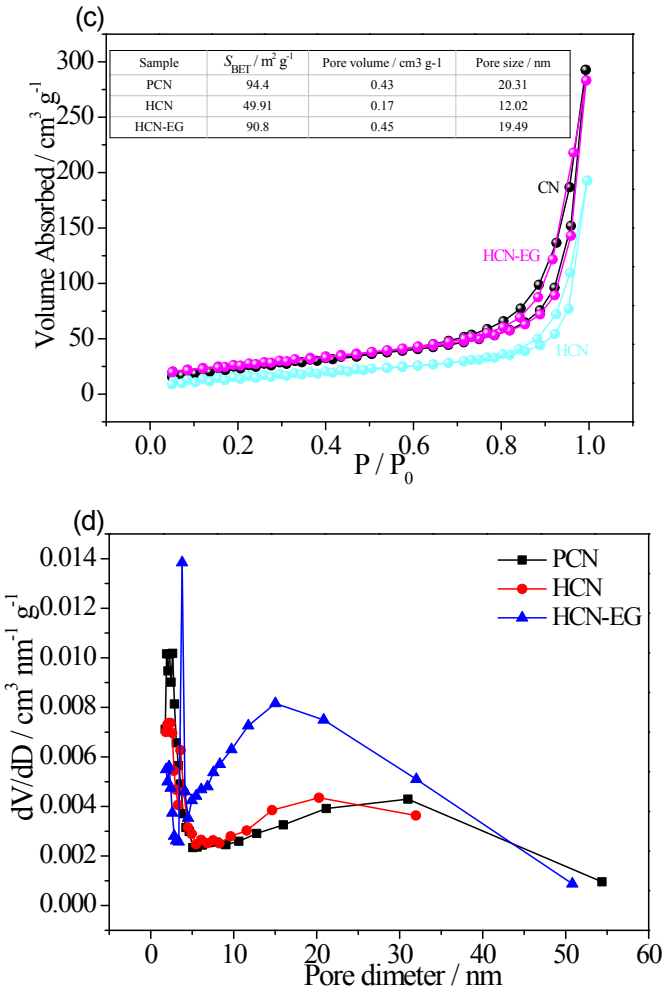

Fig. S12 Typical N_2 adsorption-desorption isotherm of samples. The specific surface area was investigated via the Brunauer-Emmett-Teller (BET) method and the pore size was studied by using Barret-Joyner-Halenda (BJH) model.

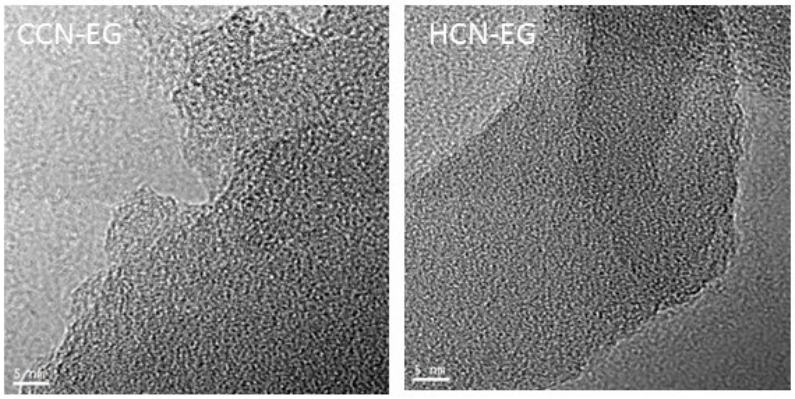

Fig. S13 Typical Transmission electron microscope images of CCN-EG and HCN-EG.

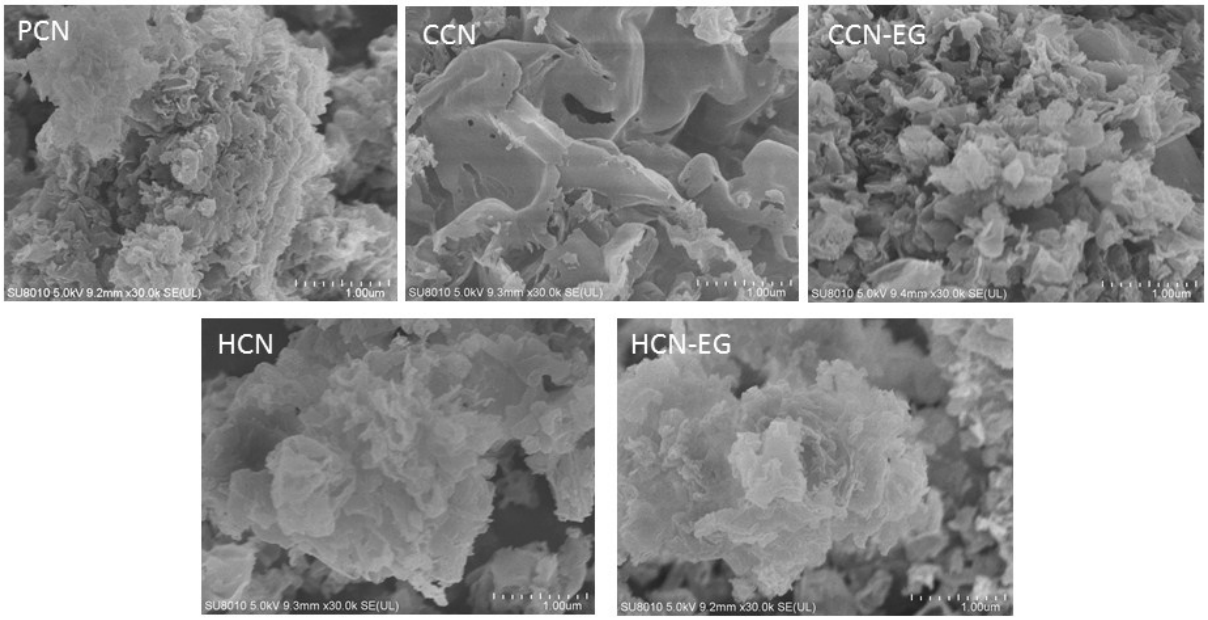

Fig. S14 The SEM images of samples.

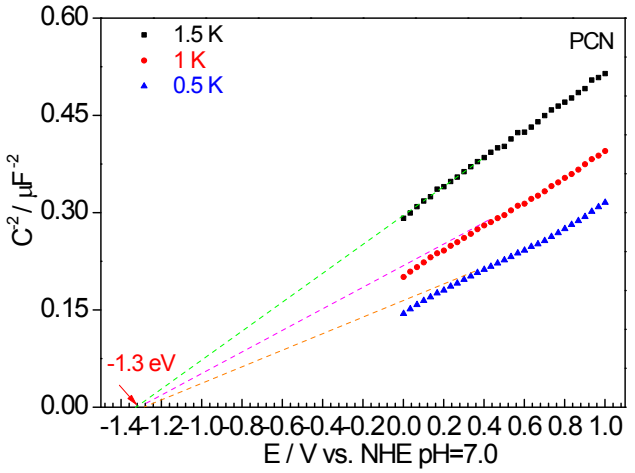

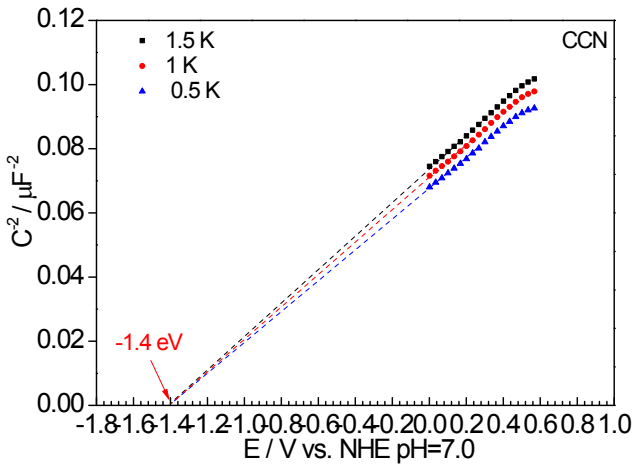

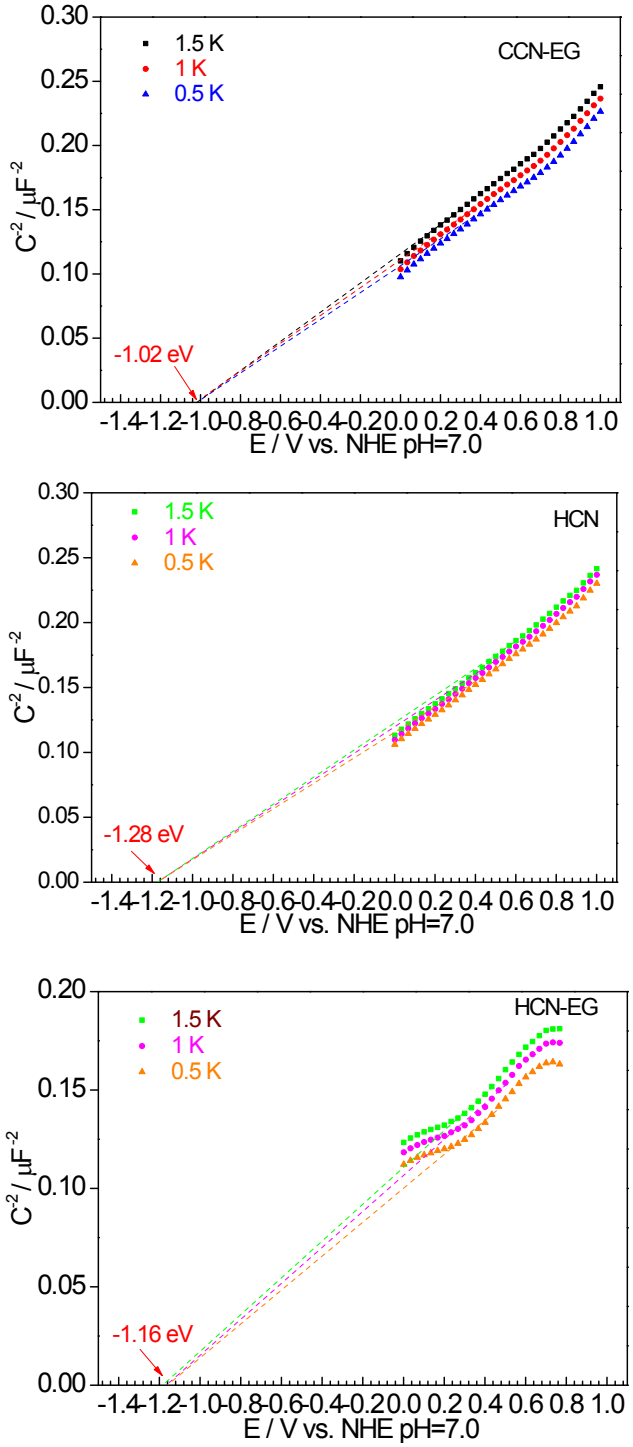

Fig. S15 Mott-Schottky plots of the samples.

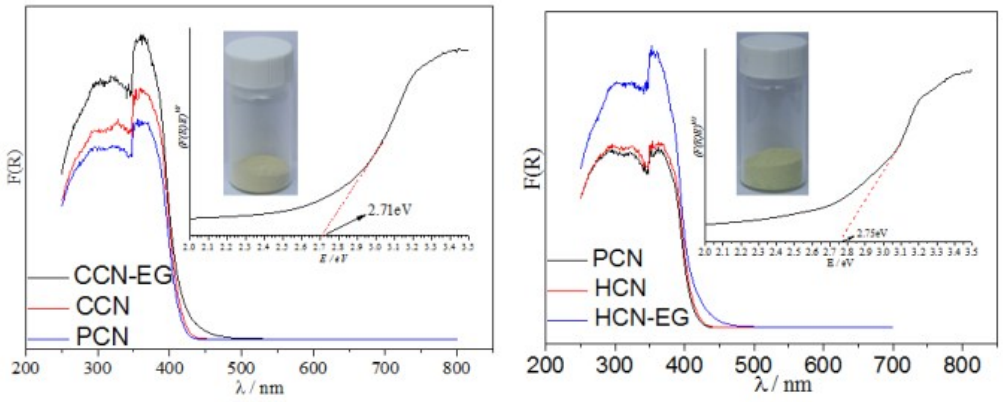

Fig. S16 UV-Vis diffuse reflectance spectra (DRS) of two types of surface chemical decoration.

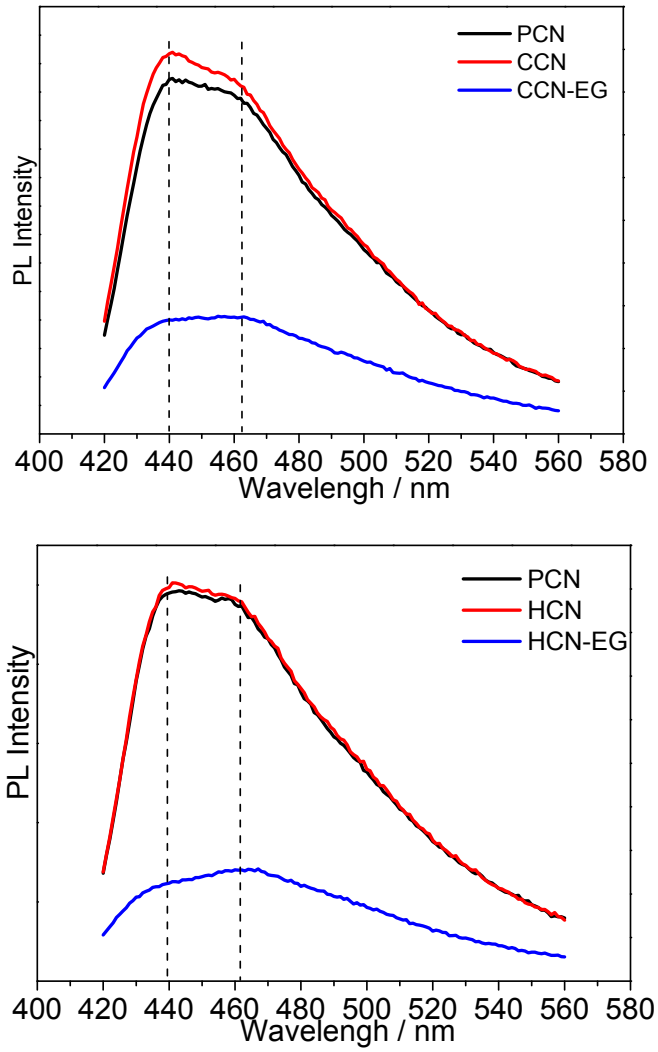

Fig. S17 PL spectra.

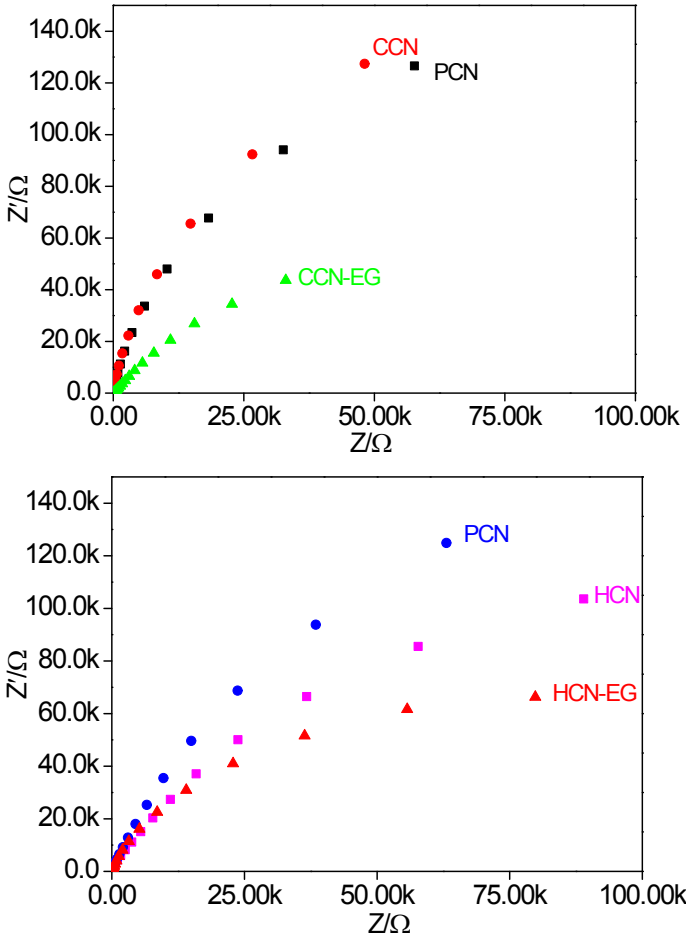

Fig. S18 Electrochemical impedance spectrum.

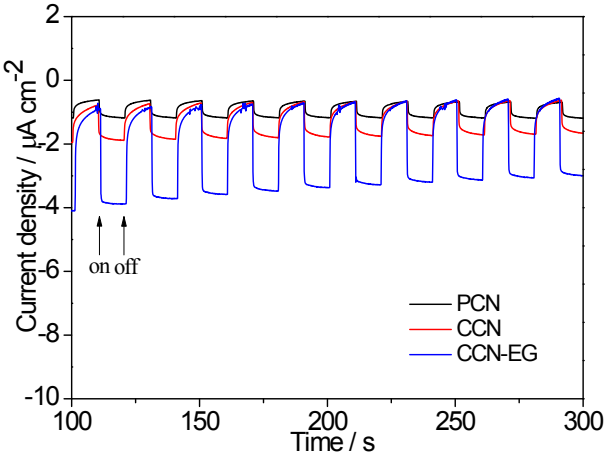

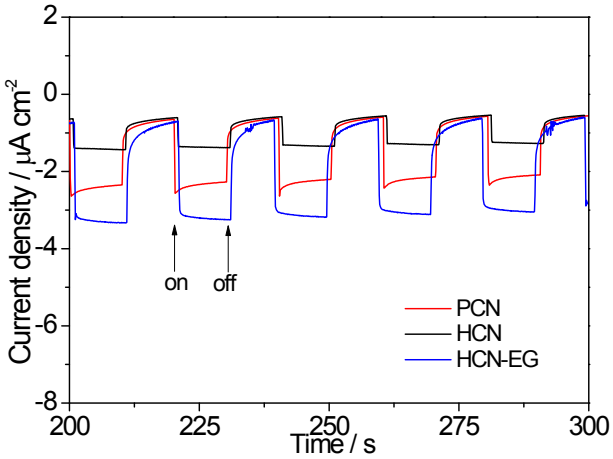

Fig. S19 Photocurrent density in chemical and hydrogen bond modified PCN.

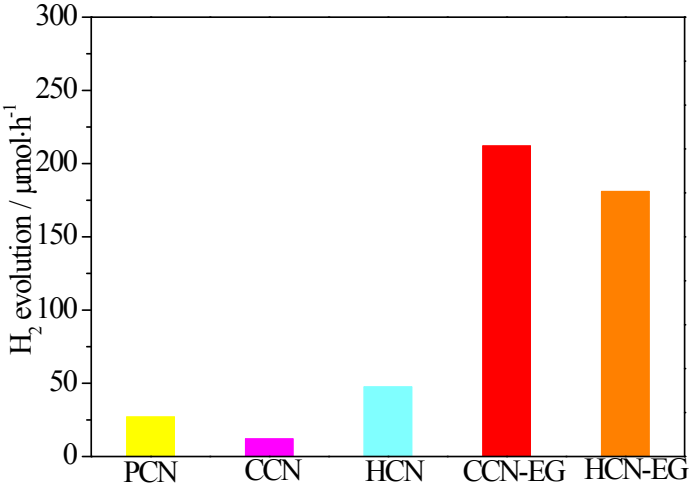

Fig. S20 The H_2 production of modified PCN

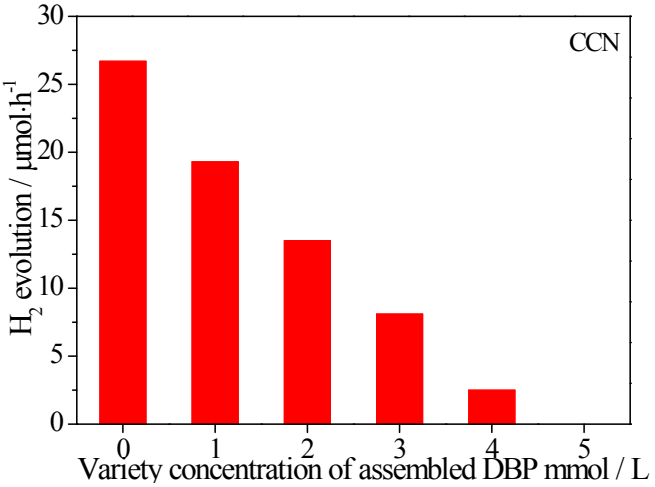

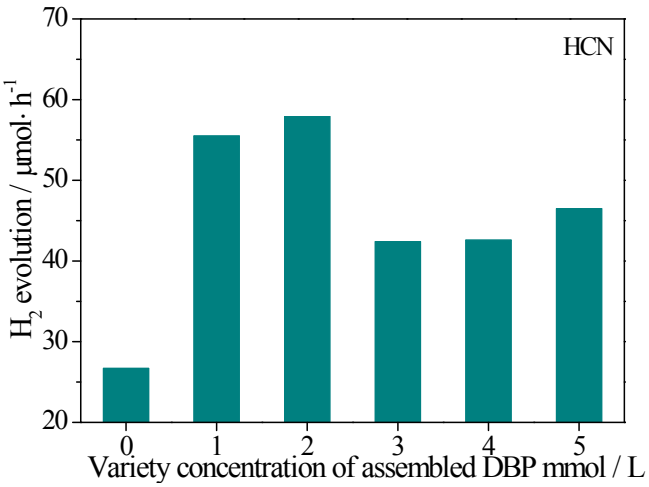

Fig. S21 The changed H_2 production after variety concentration of DBM molecules anchored upon CCN and HCN.

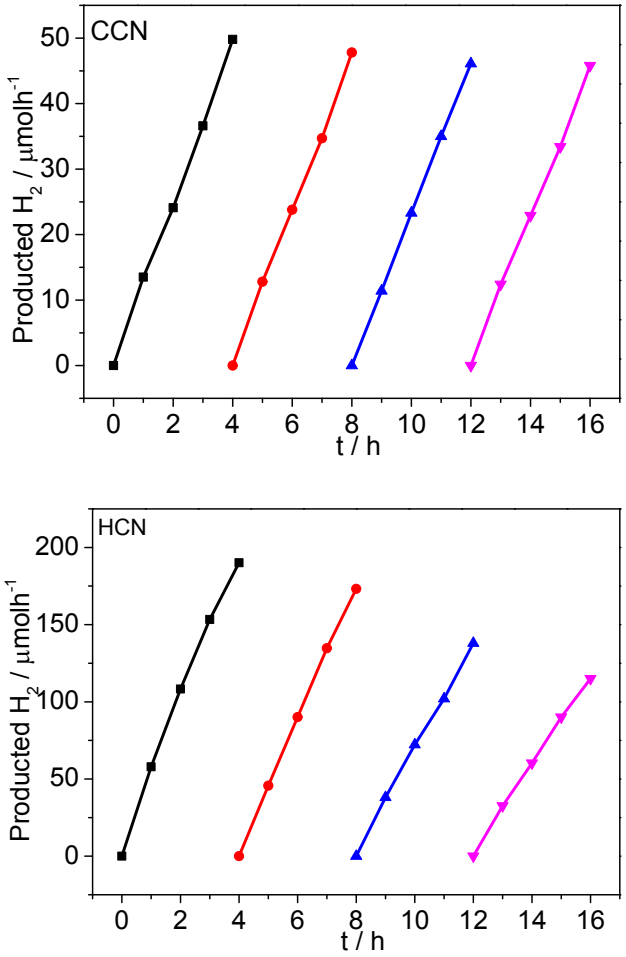

Fig. S22 Photocatalytic activity of CCN and HCN.

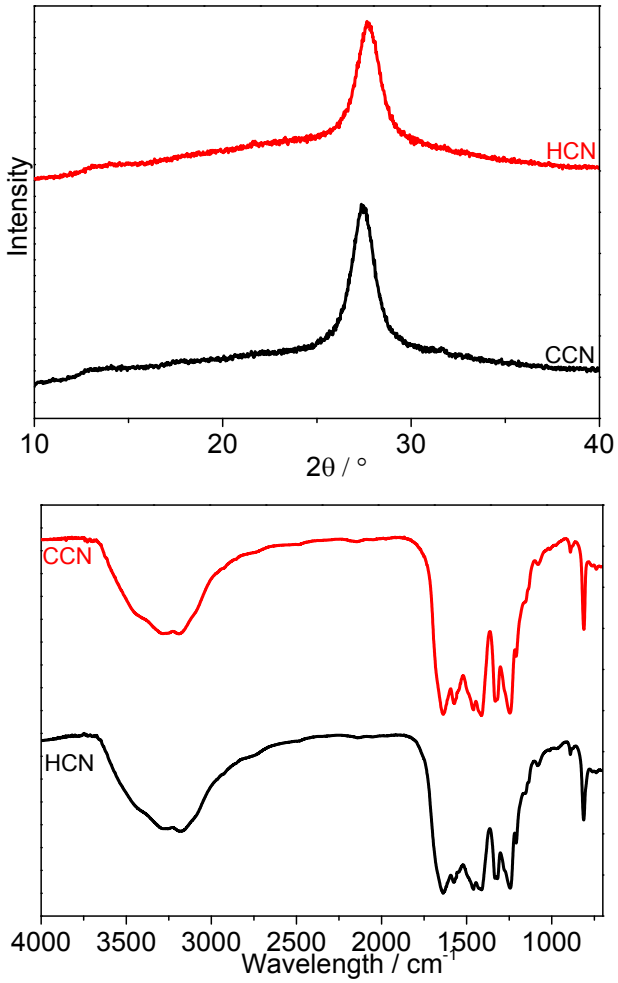

Fig. S23 XRD and FT-IR of recycled CCN and HCN.

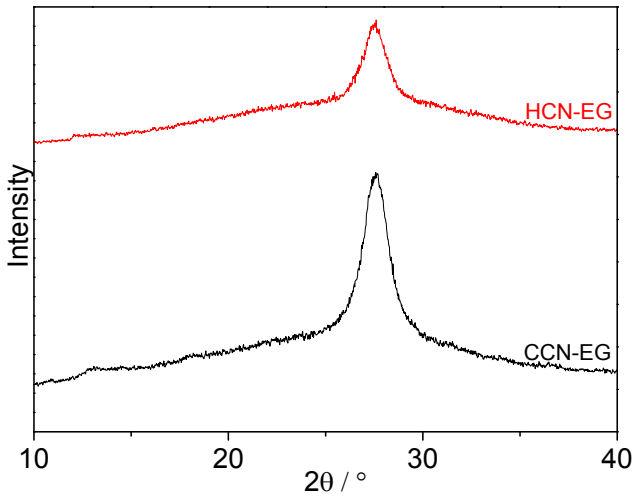

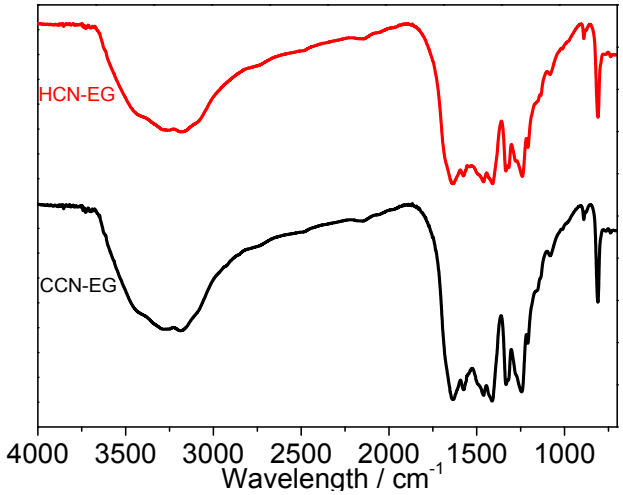

Fig. S24 XRD and FT-IR of recycled CCN-EG and HCN-EG.

Table S4. The elemental analysis (EA) results of CCN-EG, HCN-EG and recycled catalysts

	C(%)	N(%)	H(%)	C/N (atom ratio)
CCN-EG	32.54	55.27	2.80	0.68
CCN-EG - recycled	31.58	55.03	2.54	0.67
HCN-EG	32.68	53.39	2.82	0.71
HCN-EG - recycled	32.34	55.44	2.65	0.68

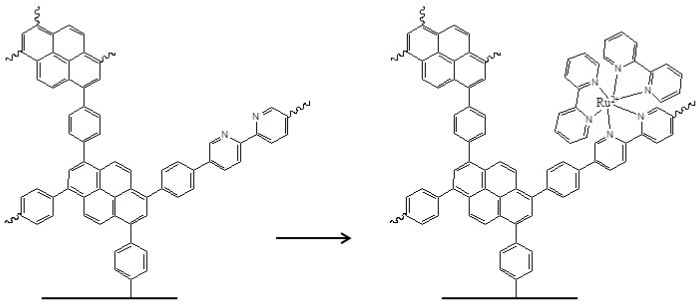

Fig. S25 Illustration of the preparation of dye modified.

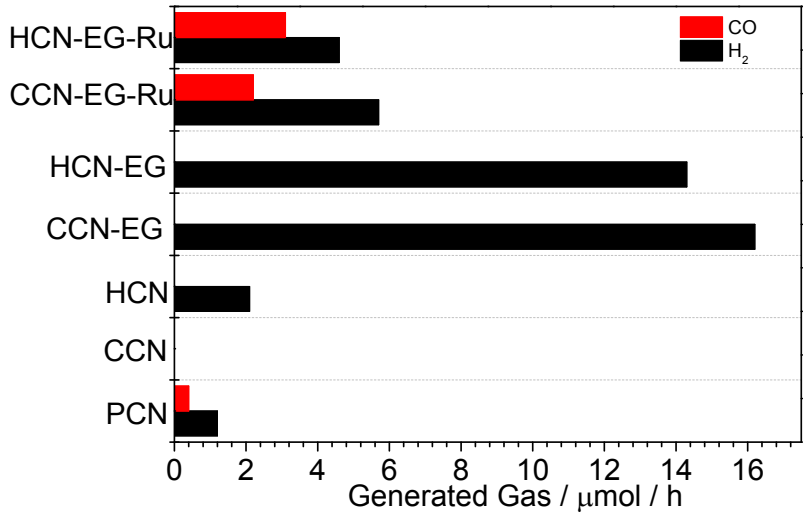

Fig. S26 Photocatalytic CO_2 reduction

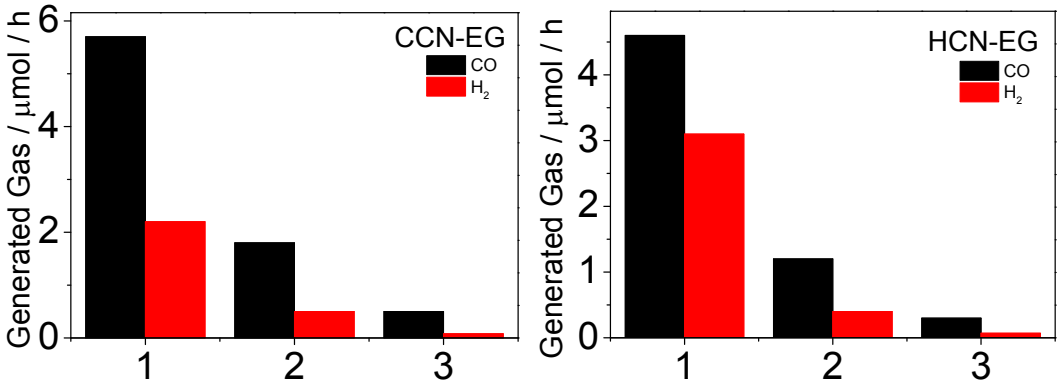

Fig. S27 The recycling text of CCN-EG and HCN-EG

References

1. O. Honghui, C. Xinru, L. Lihua, F. Yuanxing and W. Xinchen, *Angew.Chem. Int. Ed.*, 2018, **57**, 8729-8733.